Ab Initio Studies of the Dimerization of Ketene and Phosphaketene

Ulrike Salzner and Steven M. Bachrach*

Contribution from the Department of Chemistry, Northern Illinois University, DeKalb, Illinois 60115

*Received February 28, 1994. Revised Manuscript Received May 9, 1994**

Abstract: Reactants, products, and transition states for phosphaketene and ketene dimerization were optimized at the MP2/6-31G* level of theory. Single point calculations were carried out at MP4SDTQ, CCSD(T), BD, and CASSCF. 6-31G* and D95* basis sets were tested. The heat of formation of diketene is reproduced very accurately at the CCSD(T)/6-31G* level. At the same level of theory formation of diphosphetanedione is only slightly exothermic, 0.66 kcal/mol. Dimerization of ketene to yield vinylaceto-β-lactone (diketene) and 1,3-cyclobutanedione proceeds via concerted transition structures with partial charge separation. In contrast, phosphaketene dimerization reactions proceed by $[2\pi_s + 2\pi_a]$ pathways. The preferred vinylaceto-β-lactone formation during dimerization of the parent ketene is due to kinetic control. The preference for lactone over dione formation is small and dependent on the computational method. In the dimerization of phosphaketene, the dione product is more stable than the lactone product, which is in fact less stable than two isolated phosphaketene molecules. The relative activation energies for the two phosphaketene dimerization pathways are sensitive to computational level. Using perturbative methods, the dione TS is favored, but the lactone TS is favored at the CI and CASSCF(2,2) levels. The difference in the systems is analyzed in terms of geometry, strain, steric interactions, and electron distribution.

The first phosphaketene, t-BuP=C=O, was synthesized by Appel and co-workers in 1983.[1] It was prepared by the reaction of a silylphosphine with phosgene. *tert*-Butylphosphaketene is stable below –60 °C and was characterized by ^{31}P NMR and by reaction products. Above –60 °C it dimerizes to diphosphetanedione (Scheme 1), a head-to-tail cycloaddition product with a C–P–C–P ring. In contrast, phosphathioketene dimerizes to an unsymmetrical thiolactone (Scheme 2).[2] (2,4,6-Tri-*tert*-butylphenyl)phosphaketene is stable at room temperature, apparently due to the steric conjestion afforded by the bulky substituent.[3]

Phosphaketene is the phosphorus derivative of ketene. In ketene dimerization reactions only two out of four possible reaction products are observed, vinylaceto-β-lactone (diketene; **1**) and 1,3-cyclobutanedione (**2**).[4] Dimerization of the parent ketene yields about 95% vinylaceto-β-lactone, the unsymmetrical head-to-head cycloaddition product, and 4–5% 1,3-cyclobutanedione. In the absence of catalysts, the majority of substituted ketenes dimerize to 1,3-cyclobutanediones[5] and the thermodynamically less stable, that is the sterically more hindered, products are formed.[6] However, the product distribution is extremely sensitive to the reaction conditions. Diphenylketene, for instance, upon heating dimerizes to the corresponding lactone, but in the presence of CH_3ONa, the 1,3-cyclobutanedione is formed. In the presence of $AlCl_3$, lactones will rearrange to 1,3-cyclobutanediones.[5]

There is experimental and theoretical evidence that 1,3-cyclobutanedione (**2**) and diketene (**1**) are of comparable stability.[7,8] The preference for diketene formation thus appears to be due to kinetic control.

Face-to-face $[2\pi_s + 2\pi_s]$ cycloadditions (Scheme 3a) of alkenes and ketenes are symmetry forbidden according to the Woodward–

Scheme 1

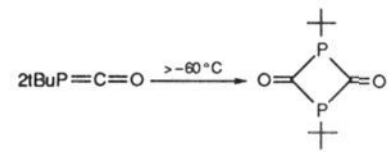

Scheme 2

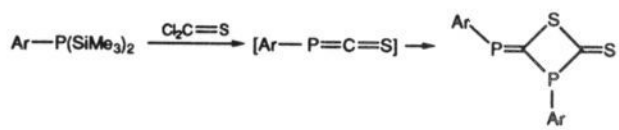

Scheme 3

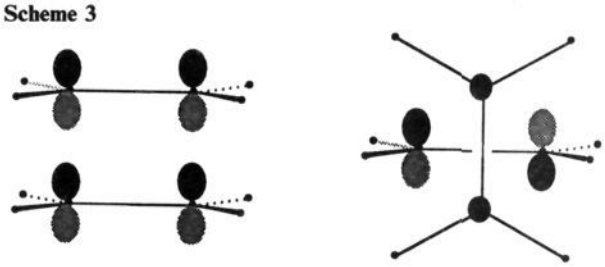

Hoffmann rules.[9] An alternative concerted $[2\pi_s + 2\pi_a]$ reaction mechanism (Scheme 3b), however, is possible[9] and provides an explanation for the formation of the more hindered product in terms of the less hindered approach in the transition state.[6] Experimental investigations support the concerted nature of the reaction. Rice and Greenberg observed that the rate of polymerization of ketene is insensitive to the presence of oxygen,[10] strongly suggesting that radical intermediates are not involved.

* Abstract published in *Advance ACS Abstracts,* July 1, 1994.

(1) Appel, R.; Paulen, W. *Tetrahedron Lett.* **1983**, *24*, 2639–2642.
(2) Appel, R.; Fölling, P.; Krieger, L.; Siray, M.; Knoch, F. *Angew. Chem., Int. Ed. Engl.* **1984**, *23*, 970.
(3) Appel, R.; Paulen, W. *Angew. Chem., Int. Ed. Engl.* **1983**, *22*, 785.
(4) Tenud, L.; Weilemann, M.; Dallwigk, E. *Helv. Chim. Acta* **1977**, *100*, 975–977.
(5) Seebach, D. In *Houben-Weyl, Methoden der Oganischen Chemie*, Thieme Verlag: Stuttgart, 1971; Vol. 4/4.
(6) Lowry, T. H.; Richardson, K. S. *Mechanism and Theory in Organic Chemistry*, 3rd ed.; Harper and Row: New York, 1987.
(7) Chickos, J. S.; Sherwood, D. E., Jr.; Jug, K. *J. Org. Chem.* **1978**, *43*, 534.
(8) Seidl, E. T.; Schaefer, H. F., III *J. Am. Chem. Soc.* **1990**, *112*, 1493–1499.
(9) Woodward, R. B.; Hoffmann, R. *Angew. Chem., Int. Ed. Engl.* **1969**, *8*, 781–853.
(10) Rice, F. O.; Greenberg, J. *J. Am. Chem. Soc.* **1934**, *56*, 2132–2134.

0002-7863/94/1516-6850$04.50/0

Huisgen and Otto investigated the solvent dependence of the rate constants for the dimerization of dimethylketene.[11] The moderate solvent dependency observed led these authors to exclude zwitterionic intermediates. Since the reaction product 2,2,4,4-tetramethyl-1,3-cyclobutanedione has no dipole moment, a reversed effect of solvent polarity is to be expected if a symmetric transition state were involved. Huisgen and Otto therefore suggested ketene dimerizations to be concerted but the transition states are highly asynchronous with partial charge separation.

The reaction mechanism of the ketene dimerization has been examined twice[12,13] by means of *ab initio* methods. At the MP2/4-31//HF/STO-3G level, Fu, Decai, and Yanbou found the reaction to be concerted and the $[2\pi_s + 2\pi_a]$ approach to be preferred over $[2\pi_s + 2\pi_s]$. The activation barrier for 1,3-cyclobutanedione formation, however, was 5 kcal/mol lower than for vinylaceto-β-lactone formation. Seidl and Schaefer[13] investigated the reaction at much higher levels of theory and revealed that the $[2\pi_s + 2\pi_s]$ "transition structure" found by Fu, Ducai, and Yanbou has three imaginary frequencies and the $[2\pi_s + 2\pi_a]$ "transition structure" has two imaginary frequencies. Seidl and Schaefer located proper transition structures at the HF/DZ+P level for the dimerization of ketene. At CISD+Q/DZ//HF/DZ, the experimental preference for vinylaceto-β-lactone formation is reproduced. The transition structures for vinylaceto-β-lactone and 1,3-cyclobutanedione formation were both found to be asynchronous as suggested by Huisgen and Otto.[11] Schaad, Gutman, Hess, and Hu[14] determined the secondary deuterium isotope effect for the dimerization of ketene to diketene using ab initio frequencies. Their transition structure is essentially identical to the one found by Seidl and Schaefer and gives isotope effects in reasonable agreement with the limited experimental data.

Bernardi and co-workers studied potential energy surfaces of cycloadditions of ketenes to alkenes at the MCSCF level. $[2\pi_s + 2\pi_a]$ transition structures have been located for various reactions and were shown to be second order saddle points.[15-17] These authors conclude that $[2\pi_s + 2\pi_a]$ transition structures do not exist in general for this type of reaction. Two pathways were shown to exist for the ketene to ethylene cycloaddition: one in which the two fragments approach each other in parallel planes and one with a perpendicular approach. Both had approximately the same energy and for both pathways intermediates were located. Ring closure to oxetane and cyclobutane is possible from these intermediates; formation of oxetane has the higher barrier.

The goal of this investigation is to examine the reaction mechanism of the phosphaketene dimerization. Transition structures for head-to-head and head-to-tail self-addition of phosphaketene are located and the applicability of the Woodard–Hoffmann rules to higher row systems is investigated. The results are discussed in comparison with the ketene dimerization. We first determine an adequate theoretical level for the parent ketene reactions 1 and 2 where experimental and theoretical data exist and then compute the phosphaketene reactions 3 and 4 (see Scheme 4) at the same level of theory. Natural bond orbital (NBO)[18-20] and topological electron density[21] analyses are employed to examine and compare the nature of the transition structures of phosphorus and carbon systems.

Table 1. Reaction and Activation Energies (kcal mol^{-1}) for the Dimerization of Ketene[a]

	reaction 1		reaction 2	
level	ΔE	E_a	ΔE	E_a
HF	-18.00	36.96	-20.26	40.23
MP2	-22.78	24.98	-23.55	22.92
MP3	-25.83	30.20	-26.44	30.43
MP4	-20.67	26.08	-22.03	23.59
CCSD	-23.77	30.16	-24.83	30.81
CCSD(T)	-23.47	27.61	-23.84	26.67
expt	-23[b]	31 ± 1[c]		

[a] All energies are based on MP2 optimized geometries (except the HF energies which are at the HF geometries) and are corrected for ZPE. [b] See ref 37. [c] See ref 7.

Scheme 4

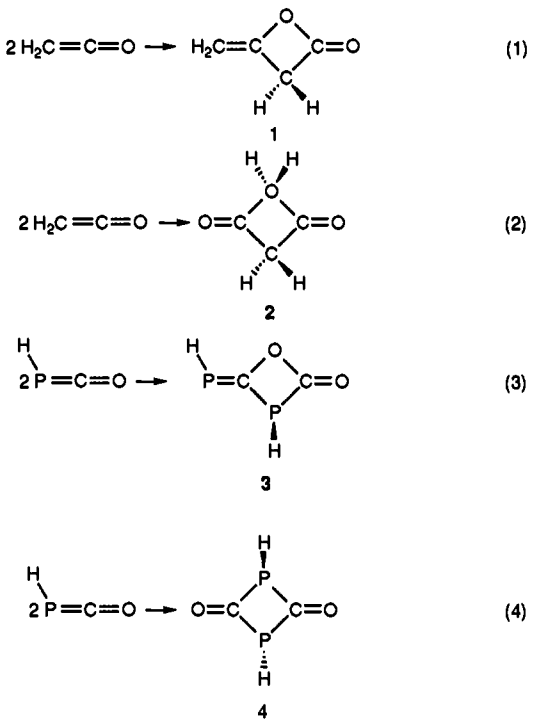

Computational Methods

Reactants, products, and transition structures for phosphaketene and ketene dimerization reactions were fully optimized at the HF/6-31G* and MP2/6-31G* levels of theory and the HF wave functions of the transition states were tested for stability. The nature of the stationary points was characterized at HF/6-31G* and that for the transition states of the ketene dimerization at MP2/6-31G*. Since these stationary points are true transition structures with one imaginary frequency at both the HF and MP2 levels, no further MP2 frequency calculations were carried out for the phosphorus analogs. In addition, single point energy calculations using the MP2 geometries were performed at the MP4SDTQ and coupled cluster singles and doubles with approximate treatment of triple excitation (CCSD(T)) levels. The energies of the transition states were also computed at CISD and Brueckner doubles (BD). The calculated reaction energies for the dimerization of ketene and phosphaketene are listed in Tables 1 and 2, respectively.

To our surprise the MP2, MP4, and CCSD(T) calculations indicate a preference for 1,3-cyclobutanedione formation by having a smaller activation energy than formation of the lactone. Most interesting is the effect of inclusion of triple excitation in the CCSD approximation. While the CCSD result is in agreement with Seidl and Schaefer's result[13] that the transition state for vinylaceto-β-lactone is lower in energy than the transition state for 1,3-cyclobutanedione, inclusion of the approximate triples contribution lowers the energy for the 1,3-cyclobutanedione formation by 1.6 kcal/mol compared to diketene formation. Therefore, complete active space (CASSCF) single point calculations seemed to be

(11) Huisgen, R.; Otto, P. *J. Am. Chem. Soc.* **1968**, *90*, 5342.
(12) Fu, X.; Decai, F.; Yanbo, D. *J. Mol. Struct. (THEOCHEM)* **1988**, *167*, 349–358.
(13) Seidl, E. T.; Schaefer, H. F., III *J. Am. Chem. Soc.* **1991**, *113*, 5195–5200.
(14) Schaad, L. J.; Gutman, I.; Hess, B. A.; Hu, J. *J. Am. Chem. Soc.* **1991**, *113*, 5200–5203.
(15) Bernardi, F.; Bottoni, A.; Olivucci, M.; Robb, M. A.; Schlegel, H. B.; Tonachini, G. *J. Am. Chem. Soc.* **1988**, *110*, 5993–5995.
(16) Bernardi, F.; Bottoni, A.; Robb, M. A.; Venturini, A. *J. Am. Chem. Soc.* **1990**, *112*, 2106–2114.
(17) Bernardi, F.; Bottoni, A.; Olivucci, M.; Robb, M. A.; Venturini, A. *J. Am. Chem. Soc.* **1993**, *115*, 3322–3323.
(18) Reed, A. E.; Weinstock, R. B.; Weinhold, F. *J. Chem. Phys.* **1985**, *83*, 735.
(19) Reed, A. E.; Weinhold, F. *J. Chem. Phys.* **1985**, *83*, 1736.
(20) Reed, A. E.; Curtiss, L. A.; Weinhold, F. *Chem. Rev.* **1988**, *88*, 899.
(21) Bader, R. F. W. *Atoms in Molecules—A Quantum Theory*; Oxford University Press: Oxford, 1990.

Table 2. Reaction and Activation Energies (kcal mol^{-1}) for the Dimerization of Phosphaketene[a]

	reaction 3		reaction 4	
level	ΔE	E_a	ΔE	E_a
HF	8.09	40.72	1.51	38.46
MP2	3.91	29.55	2.76	24.08
MP3	-0.16	35.03	-2.91	31.04
MP4	6.49	29.77	4.47	23.98
CCSD	1.19		-1.83	
CCSD(T)	2.20		-0.14	

[a] All energies are based on MP2 optimized geometries (except the HF energies which are at the HF geometrics) and are corrected for ZPE.

indicated. The active space for the CASSCF calculations was determined with the help of the coupled cluster amplitudes and included either 2 electrons and 2 orbitals (CASSCF(2,2)) or 6 electrons and 6 orbitals (CASSCF(6,6)). In addition, the effect of basis set extension has been probed by employing the Dunning 95* basis set as implemented in GAUSSIAN 92. These calculations were performed for the transition states of reactions 1 and 2 only.

All energy values are corrected for zero point vibration employing the HF/6-31G* frequencies scaled by a factor of 0.89.[22] All calculations were carried out using GAUSSIAN 92.[23]

Electronic structure analyses were carried out with the NBO program[18-20] which is implemented in L607 of GAUSSIAN 92. Topological electron density analysis was used to obtain atomic charges, bond orders, and topological bond path networks. The value of the electron density at the bond critical point $\rho(r_c)$ correlates with bond order according to the empirical formula[24,25]

$$\text{bond order} = e^{A(\rho(r_c)\cdot B)} \quad (5)$$

with A and B being empirical constants 6.458 and 0.252, respectively, for C–C[26] bonds and 19.628 and 0.153, respectively, for C–P bonds.[27] Charges were calculated with the program PROAIM[28] or VECSURF and ATOMICI.[29,30] Topological bond path networks were obtained by tracing $\nabla\rho$ from the bond critical point to the neighboring nuclei. These paths are called bond paths[31] and reflect a ridge of maximum density between atoms. Bond paths are typically in a 1:1 correspondence with chemical bonds.

Results

Geometries. The MP2/6-31G* geometries of the products of reactions 1–4 are drawn in Figure 1. Seidl and Schaefer[8,32] have argued that the experimental X-ray crystal[33] structure of **1** is inaccurate, since there are dramatic disagreements between their calculated HF/DZ+P and CCSD/DZd structures and the crystal structure. Optimization at the MP2 level does not resolve these discrepancies. In general the MP2 bond distances have lengthened a small amount relative to the HF geometry and are quite similar to the values found for the CCSD structure. However, the MP2 structure significantly differs from the X-ray structure in the C—O bond distance adjacent to the C=C bond (MP2, 1.417 Å; X-ray, 1.47 Å) and the C—C bond adjacent to the C=C bond (MP2, 1.502 Å; X-ray, 1.54 Å). We concur with Seidl and Schaefer that the X-ray structure of diketene should be re-examined. Further, the close agreement between our MP2 structure and Seidl and Schafer's CCSD structure indicates that limiting our calculations to the MP2 level should result in quite reasonable structures.

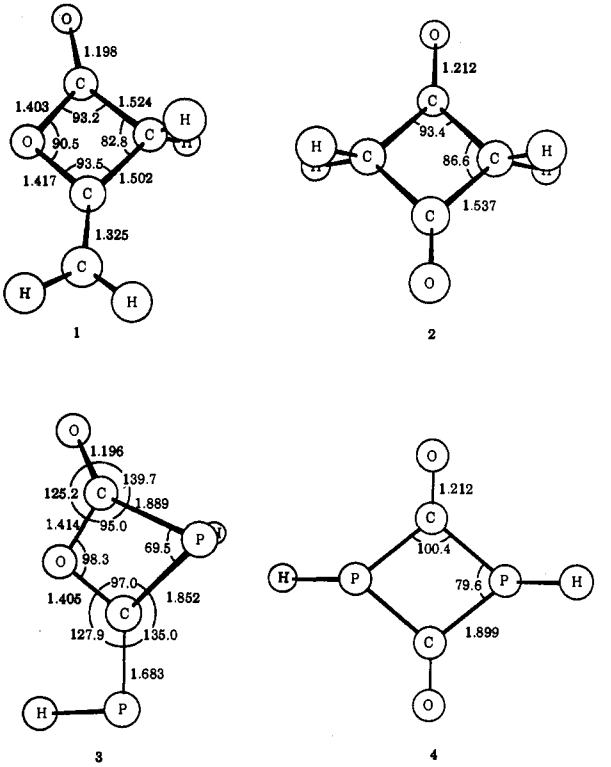

Figure 1. MP2/6-31G* optimized geometries of **1–4**. All distances are in Å and all angles are in deg.

The HF/DZ+P and MP2/6-31G* geometries of **2** differ only slightly, and in the expected sense. The bonds are longer in the correlated structure—the C=O bond is 0.029 Å longer and the C—C bond is 0.003 Å longer in the MP2 geometry.

There are no experimental structures of **3** or **4**. The *tert*-butyl derivative of **3** has been isolated and identified, but no structural information is available. We can compare the structures of these phosphorus derivatives with their parent compounds **1** and **2**. Unlike **1**, **3** is not a planar molecule. The four-membered ring is slightly puckered; the C–O–C–P dihedral angle is only 3.4°. The exocyclic double bonds are of typical length. The C–O single bonds in the ring are of comparable length to the corresponding bonds in **1**. The C–P bonds are somewhat longer than usual, particularly the bond adjacent to the carbonyl group. The major difference between **1** and **3** is the interior angles of the ring. Since phosphorus readily accommodates small angles,[34,35] the angle about P in **3** is only 69.5°, allowing the angles about the other ring atoms to expand. For example, the angle at the ring oxygen is 7.8° larger in **3** than in **1**.

Similar comparisons are drawn between **2** and **4**. Due to the pyramidal nature of phosphorus, **4** has only C_2 symmetry, but the ring is planar, just like in **2**. The C=O bond lengths are identical in the two structures. The C–P bond is long, even longer than the C–P bonds in **3**. The small angle at the two ring phosphorus atoms in **4** allows the angle about the two carbons to expand to 100.4°, much less strained than the carbonyl carbons in **2**.

The structures of the transition states for reactions 1–4 (labeled **TS1-TS4**) are shown in Figure 2. In each transition state, the ketene and phosphaketene fragments approach each other in perpendicular planes. Such approaches have also been described

(22) Hehre, W. J.; Radom, L.; Schleyer, P. v. R.; Pople, J. A. *Ab Initio Molecular Orbital Theory*; John Wiley: New York, 1986.
(23) Frisch, M. J.; Trucks, G. W.; Head-Gordon, M.; Gill, P. M. W.; Wong, M. W.; Foresman, J. B.; Johnson, B. G.; Schlegel, H. B.; Robb, M. A.; Replogle, E. S.; Gomperts, R.; Andres, J. L.; Raghavachari, K.; Binkley, J. S.; Gonzalez, C.; Martin, R. L.; Fox, D. J.; Defrees, D. J.; Baker, J.; Stewart, J. J. P.; Pople, J. A. Gaussian, Inc.: Pittsburgh, PA, 1992.
(24) Bader, R. W. F.; Tang, T. H.; Tal, Y.; Biegler-Koenig, F. W. *J. Am. Chem. Soc.* **1982**, *104*, 946–952.
(25) Bader, R. W. F.; Slee, T. S.; Cremer, D.; Kraka, E. *J. Am. Chem. Soc.* **1983**, *105*, 5061–5068.
(26) Slee, T. S. In *Modern Models of Bonding and Delocalization*; Liebman, J. F., Greenberg, A., Eds.; VCH Publishers: New York, 1988; p 69.
(27) Bachrach, S. M. *J. Mol. Struct. (THEOCHEM)* **1992**, *255*, 207–219.
(28) Biegler-Konig, F. W.; Bader, R. F. W.; Tang, T. H. *J. Comput. Chem.* **1982**, *3*, 317–328.
(29) Cioslowski, J. *Chem. Phys. Lett.* **1992**, *194*, 73–78.
(30) Cioslowski, J.; Nanayakkara, A.; Challacombe, M. *Chem. Phys. Lett.* **1993**, *203*, 137–142.
(31) Runtz, G. R.; Bader, R. F. W.; Messer, R. R. *Can. J. Chem.* **1977**, *55*, 3040–3045.
(32) Seidl, E. T.; Schaefer, H. F. I. *J. Phys. Chem.* **1992**, *96*, 657–661.
(33) Kay, M. I.; Katz, L. *Acta Crystallogr.* **1958**, *11*, 897.
(34) Bachrach, S. M. *J. Phys. Chem.* **1989**, *93*, 7780–7784.
(35) Bachrach, S. M. *J. Org. Chem.* **1991**, *56*, 2205–2209.

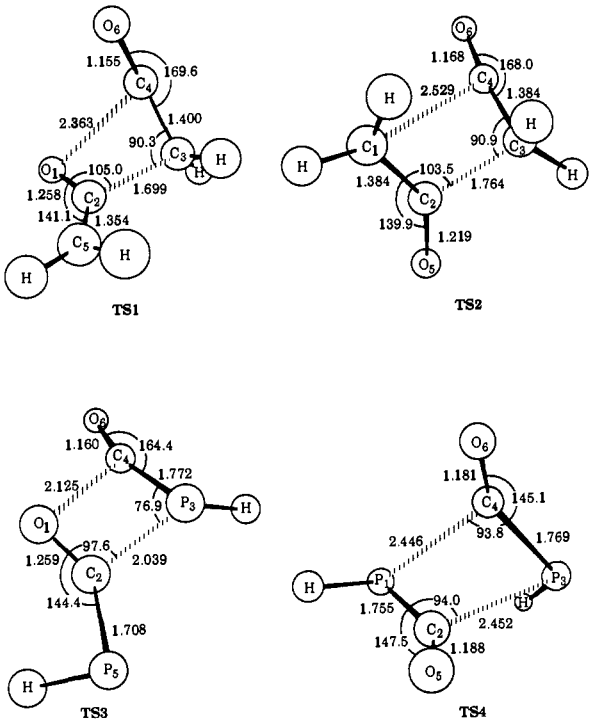

Figure 2. MP2/6-31G* optimized geometries of **TS1**–**TS4**. All distances are in Å and all angles are in deg.

for the ketene to ethylene cycloaddition. We were, however, not able to locate additional transition structures for parallel approaches also found by Bernardi et al.[16]

(a) TS1. Seidl and Schaefer[13] optimized the structure of **TS1** at HF/DZ+P. The found a transition state having no symmetry and not corresponding to a $[2\pi_a + 2\pi_a]$ or a $[2\pi_a + 2\pi_s]$ path. Our optimized geometry has a similar overall structure to the HF geometry. The ketene fragment which reacts at the terminal carbon is nearly linear while the other ketene fragment is quite bent [$\Theta(O_1–C_2–C_5) = 141.1°$]. The $O_1–C_2–C_3–C_4$ dihedral angle is −54.3°, compared to −55.7° at HF/DZ+P. There are a few significant differences. The forming $C_2–C_3$ bond is quite short, 1.699 Å at MP2. This is 0.063 Å shorter than in the HF geometry, and only 0.192 Å larger than in **1**. The $O_1–C_4$ distance is 0.310 Å shorter in the MP2 structure than in the HF structure. The transition state is clearly much later on the MP2 surface than on the HF surface.

(b) TS2. As above, there is general agreement in the overall structure of **TS2** at HF[13] and MP2. The structure has no symmetry. The $C_2–C_3$ distance is 0.151 Å longer in the MP2 structure than the HF structure. The $C_1–C_4$ distance is unaffected by correlation and is very long, indicating little bonding interaction has developed in this TS. The $C_1–C_2–C_3–C_4$ dihedral angle is 61.5° at MP2 and 53.4° at HF. The only significant difference between the HF and MP2 structures is the degree of reaction that has occurred at the C_3-containing ketene fragment. The $C_3–C_4$ distance is 0.036 Å longer in the MP2 geometry and the $C_3–C_4–O_6$ angle is 6.6° smaller than in the MP2 structure, suggesting that the MP2 TS is somewhat later along the reaction pathway than the HF TS.

(c) TS3. The geometry of **TS3** is similar to that of **TS1**. In both cases, the bond formation is asynchronous. In **TS3** the $C_2–P_3$ bond is only 0.187 Å longer than in the product. The forming $C_1–O_4$ bond is long (2.125 Å), but this is much shorter than the $C_1–O_4$ distance in **TS1**. The degree of bending about the allene carbon of each phosphaketene fragment in **TS3** is similar to the bending in the analogous ketene fragment of **TS1**; i.e. there is one fragment that is nearly linear and one that is bent to about 142°. The $O_1–C_2–P_3–C_4$ dihedral angle is 40.5°. The geometry of **TS3** may be consistent with a $[2\pi_s + 2\pi_a]$ pathway, depending on the bond orders of the forming C–P and C–O bonds. We will address this point later on.

Table 3. Relative Energies (kcal mol^{-1}) of Transition Structures for Ketene and Phosphaketene Dimerization Reactions at Various Levels of Theory, Corrected for ZPE

	$E_{TS2} - E_{TS1}$		
level	6-31G*	D95*	$E_{TS4} - E_{TS3}$
HF	+3.27	+4.88	−1.38
MP2	−2.06	−1.09	−5.48
MP3	+0.22	+2.08	−3.99
MP4(SDTQ)	−2.49	+0.98[a]	−5.79
CI	+2.08	+3.1[b]	+0.43
CCSD	+0.65	+1.62	
CCSD(T)	−0.94	+0.57	
BD	+0.80		
CASSCF(2,2)	+4.97		+5.25
CASSCF(6,6)	+6.24		

[a] MP4SDQ. [b] CISD/DZ+d/HF/DZ+P see ref 13.

(d) TS4. The structure of **TS4** is quite different than the other transition states. The two forming C–P bonds are of nearly equal distance: 2.446 and 2.452 Å. The phosphaketene fragments are both bent with Θ(P–C–O) values of 145.1° and 147.5°. The P–C–P–C dihedral angle is −50.9°. This geometry is consistent with a $[2\pi_s + 2\pi_a]$ pathway.

Energies. The reaction and activation energies for reactions 1 and 2 are presented in Table 1. The values of ΔE using the 6–31G* basis set are about 1 kcal mol^{-1} less exothermic than the results obtained using the DZ+P or DZd basis set.[13] Inclusion of electron correlation increases the exothermicity of each reaction. Our best calculation, CCSD(T)/6-31G*//MP2/6-31G*, gives the energy of reaction within 0.5 kcal mol^{-1} of the experimental value, an improvement in agreement over the best previous calculation. Our results are in agreement with Seidl and Schaefer in that **2** is lower in energy than **1** at all levels of theory. Therefore, product formation is not thermodynamically controlled.

Reaction 3 becomes more exothermic with the inclusion of electron correlation (see Table 2). At the HF level the reaction is endothermic (ΔE = 8.09 kcal mol^{-1}) but this is reduced to 2.20 at CCSD(T). On the other hand, the reaction energy of reaction 4 is larger at the MP2 (2.76 kcal mol^{-1}) and MP4 (4.47 kcal mol^{-1}) levels relative to the HF (1.51 kcal^{-1}) result. However, the CCSD(T) reaction energy (−0.14 kcal mol^{-1}) is lower than the HF result. At all computational levels, **4** is lower in energy than **3**, which is consistent with thermodynamic control in the experiments. Interestingly, the dimerization of phosphaketene to **3** is endothermic, while dimerization to **4** is essentially thermoneutral, in contrast to the large exothermicity for dimerization of ketene to either **1** or **2**.

The activation energy of reaction 1 ranges from 25 to 30 kcal mol^{-1} at the correlated levels, which is somewhat lower than the experimental[7] value of 31 kcal mol^{-1}. However, in discrepancy with experiment, the MP calculations predict that the activation barrier is lower for reaction 2 than for reaction 1. This is also contrary to Seidl and Schaefer's calculations.[13] We therefore examined the difference in the energies of the two transition states **TS1** and **TS2** using a variety of different computational levels and basis sets. These results are collected in Table 3. Examination of this table leads to a few conclusions. First, the variational methods suggest that **TS1** is lower in energy than **TS2**. Seidl and Schaefer's CISD and CCSD calculations placed **TS2** about 3 kcal mol^{-1} above **TS1**. While our results place them closer in energy, the preference for **TS1** is increased with the larger D95* basis set. It should be noted that these correlated energy differences are *smaller* than the difference at the HF level. The only exception is our CCSD(T)/6-31G* result where **TS2** is 0.65 kcal mol^{-1} lower in energy than **TS1**. Second, inclusion of nondynamical correlation favors **TS1** over **TS2**. **TS1** is lower in energy than **TS2** in both CASSCF calculations than at the HF level. Finally, the perturbational methods favor **TS2**. Clearly,

Table 4. Topological Electron Density Properties at Bond Critical Points in the Transition States

TS1			TS2		
bond	$\rho(r_c)^a$	BO[b]	bond	$\rho(r_c)^a$	BO[b]
O_1–C_2	0.385		C_1–C_2	0.321	1.56
C_2–C_3	0.166	0.57	C_2–C_3	0.146	0.50
C_3–C_4	0.279	1.19	C_3–C_4	0.291	1.29
C_2–C_5	0.332	1.68	C_2–O_5	0.412	
C_4–O_6	0.466		C_4–O_6	0.453	
TS3			**TS4**		
bond	$\rho(r_c)^a$	BO[b]	bond	$\rho(r_c)^a$	BO[b]
O_1–C_2	0.379		P_1–C_2	0.148	0.91
C_2–P_3	0.120	0.52	C_2–P_3	0.054	0.14
P_3–C_4	0.138	0.74	P_3–C_4	0.142	0.81
O_1–C_4	0.050		P_1–C_4	0.052	0.14
C_2–P_5	0.165	1.27	C_2–O_5	0.434	
C_4–O_6	0.459		C_4–O_6	0.439	

[a] Value of the electron density (e au^{-3}) at the bond critical point. [b] Bond order derived from eq 5.

the energy difference between the two transition states is sensitive to the computational method employed.

Since the variational and CASSCF calculations favor **TS1** we believe that large multireference CI calculations will result in **TS1** being the lower energy transition state. Keep in mind that all calculations were performed using the MP2 geometries, a method that favors **TS2**. In other words, it is likely that full geometry optimization at one of the variational levels will result in an even greater stability of **TS1** relative to **TS2**. Nevertheless, the energetic effect of electron correlation is small.

We now examine the dimerization of phosphaketene. Unlike the hydrocarbon system, the activation energy for formation of the dione product **4** is lower in energy than for formation of the lactone **3** at the HF level. Inclusion of electron correlation using perturbational methods further lowers the energy of **TS4** over **TS3**. On the other hand, the relative energies are reversed at the CI and CASSCF(2,2) levels. Unfortunately, the size of these systems precludes calculations at higher levels. We therefore cannot firmly resolve the relative ordering of **TS3** and **TS4**. Nevertheless, while **3** may be the kinetic product, depending on which computational level is chosen, the observed product **4** is the thermodynamic product.

Electronic Structures of the Transition States. Mulliken, natural, and Bader populations within the ketene and phosphaketene fragments differ considerably. However, all three population analyses agree in the amount of charge shifted from one ketene (phosphaketene) fragment to the other in the transition structures. The values are 0.4–0.5 e for reaction 1, 0.3–0.4 e for reaction 2, 0.5–0.6 e for reaction 3, but only 0.0–0.1 e for reaction 4. Thus, charge transfer in the transition states for reactions 1–3 is right in between what would be expected for biradicaloid and zwitterionic reaction mechanisms. These reactions then may be designated as biradicaloid with partial charge separation. There is essentially no charge transfer present in **TS4**.

Natural bond orbital (NBO) analyses of the transition structures **TS1** and **TS2** indicate that the C_2–C_3 bonding orbitals are occupied by 1.85 and 1.83 e, respectively. The bonds are polarized toward C_3, that is 65% of the bonding orbital is located on C_3. The π-bonds between C_2 and O_1 and between C_2 and O_5 are broken in both TSs, respectively. There is only a single bond left between C_3 and C_4, whereas C_4 and O_6 are triply bonded, although these triple bonds are strongly polarized toward O. This agrees with the fact that these C–O bonds are shortened (1.155 and 1.168 Å) compared to those in ketene (1.180 Å), diketene (1.198), and 1,3-cyclobutanedione (1.212 Å). No bonding interactions are present between C_1 and O_4 in **TS1** nor between C_1 and C_4 in **TS2**. The above NBO results are in perfect agreement with Bader analyses. The C_2–C_3 bond orders, according to eq 5, in **TS1** and **TS2** are 0.57 and 0.50, respectively,

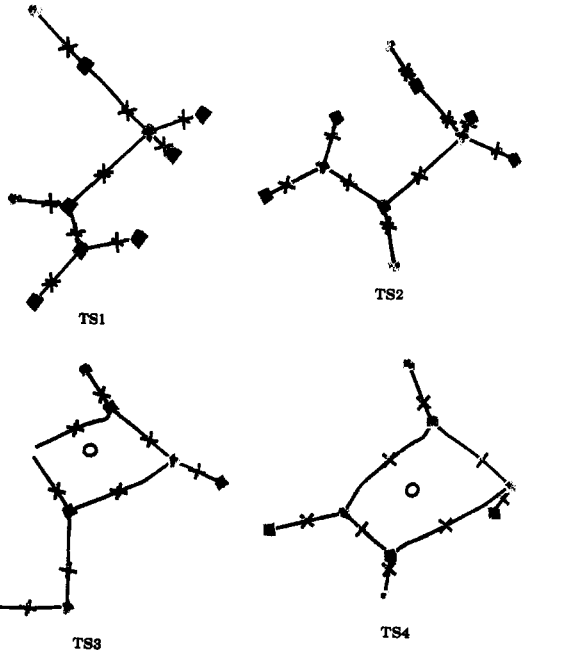

Figure 3. Topological bond path networks for the transition states **TS1**–**TS4**. The molecules are oriented as shown in Figure 2. Bond and ring critical points are denoted by ✱ and O, respectively.

indicating about half-formed bonds. The bond orders for the C_3–C_4 bonds are 1.19 in **TS1** and 1.29 in **TS2**, suggesting that the π-bond is nearly gone. The bond path network for these transition structures is in Figure 3. There is no bond critical point between C_1 and O_4 in **TS1** nor between C_1 and C_4 in **TS2**, and, therefore, no ring critical point. The electronic distribution suggests asynchronous bond forming/breaking for both reactions 1 and 2.

NBO and Bader analyses indicate that the character of the transition structures **TS3** and **TS4** for the phosphaketene dimerizations is fundamentally different from that of **TS1** and **TS2**. The forming C_2–P_3 bond in **TS3** is quite far developed, with an occupancy of 1.89 e (NBO) and a bond order of 0.52 (according to eq 5). NBO analysis reveals a strong interaction between O_1 and C_4. Bader analysis confirms this interaction: a bond critical point is found between O_1 and C_4 with $\rho(r_c) = 0.050$ e au^{-3}. We cannot estimate the bond order of the C–O bonds, due to a lack of parameterization. For comparison, the value of $\rho(r_c)$ for the C–O bonds in **1** and **3** ranges from 0.261 to 0.278 e au^{-3}. The topological bond path network for **TS3** (Figure 3) shows a four-membered ring with a ring critical point.

The two forming P–C bonds in **TS4** have nearly identical electronic properties. Their NBO occupancies are 1.758 and 1.784 e, while their bond orders (determined using eq 5) are 0.14. The breaking P–C bonds have bond orders of 0.91 and 0.81. The topological bond path network of **TS4** shows a symmetrical four-membered ring with a ring critical point. **TS3** and **TS4** are topologically identical and distinct from **TS1** and **TS2**. These results suggest that the phosphaketene dimerizations are more synchronous than the ketene dimerizations. Furthermore, **TS4** is so symmetrical as to strongly suggest a truly synchronous reaction.

Discussion

Diketene (**1**) and 1,3-cyclobutanedione (**2**) are very close in energy. Experimental reaction enthalpies of around 23 kcal/mol for the ketene dimerization are accurately reproduced at the CCSD(T)/6-31G* level of theory and **2** is predicted to be more stable than **1** at all levels of theory. This is consistent with the previous theoretical studies of Seidl and Schaefer.[8] In contrast, the dimerization of phosphaketene to give **4** is predicted to be only slightly exothermic according to our best calculations. At

all levels of theory, **4** is lower in energy than the lactone product **3**. This result is in agreement with experimental observation of the diketone product only. The preference of **4** over **3** can be simply understood in terms of ring strain energy. Phosphorus is better able to accommodate the small angles in these rings than the first-row atoms.

That the dimerization of phosphaketene is less exothermic than the dimerization of ketene is somewhat puzzling. The P–C π-bond is weaker than the C–C π-bond. The products **3** and **4** should be less strained than **1** or **2** due to the incorporation of phosphorus into the ring. Cumulenes are typically very reactive, oftentimes justified by a "strain" associated with the carbon forming the two double bonds. Relief of this strain drives the dimerization of ketene. However, the electronic structure and geometry of phosphaketene is quite different from ketene. Phosphaketene has a bent backbone [Θ(P–C–O) = 174.4°]. The C–O distance is shorter in phosphaketene (1.174 Å) than in ketene (1.180 Å). The value of $\rho(r_c)$ for the P–C bond is only 0.1505 e au^{-3}, which corresponds to a bond order of only 0.95. Further, the value of $\rho(r_c)$ for the C–O bond is 0.448 e au^{-1}, which is larger than for the C–O bond in ketene (0.439 e au^{-3}). Nguyen, Hegarty, and McGinn[36] have argued that phosphaketene contains a dative bond between PH and CO, supported by π-back-donation. This suggests that the carbon in phosphaketene is less strained (making π-bonds to just the oxygen) than in ketene, and is consequently less reactive.

Activation energies for phosphaketene dimerizations are about 3 kcal higher than those for ketene dimerizations at comparable levels of theory. This probably reflects the greater exothermicity of the ketene dimerization reactions. The energy differences between lactone and dione formation transition structures are small for both systems. The relative energies are sensitive to improvement of basis sets and correlation treatment. Basis set improvement and inclusion of non-dynamical correlation preferentially lowers the activation energy for lactone formation. Perturbation expansion of the correlation energy prefers the dione product. It is likely that definitive estimates of the relative activation energies will require multireference CI calculations with large basis sets. The general sense of these calculations is that the activation energy is lower for formation of **1** than for formation of **2**, indicating that kinetic control is indeed responsible for the diketene formation. For phosphaketene dimerization, the relative activation energy for formation of **3** and **4** is dependent on the computational method, with perturbational methods favoring **TS4** while CI and CASSCF methods favor **TS3**. Thus, the diphosphadione product is the thermodynamic product and may also be the kinetic product.

Finally, we address the nature of the reaction course. Previous experimental[11] and theoretical[13] studies concluded that ketene dimerizations do not proceed via [$2\pi_s + 2\pi_a$] pathways. Rather a polar diradicaloid transition state was proposed. Our calcultions fully support this conclusion for both reaction pathways (reactions 1 and 2). The geometry of **TS1** and **TS2** shows a relatively close distance separating C_2 and C_3 and no bonding interaction between the other two atoms that will join in the product. Both NBO and the topological method concur in finding considerable bonding developed between C_2 and C_3 and no ring formation in the transition state. The reactions clearly are highly asynchronous.

The pathway for the dimerization of phosphaketene is decidedly different than that for ketene. Comparing the geometry of **TS1** and **TS3**, we note an O_1–C_4 distance that is 0.24 Å shorter in the latter. This shorter distance reflects the presence of a partial bond between these atoms in **TS3** that is not present in **TS1**, resulting in topological ring structure in **TS3** but not in **TS1**. It is difficult to judge the degree of synchronicity in **TS3** without having the bond orders of the C–O bonds, but clearly reaction 3 is more synchronous than reaction 1. The transition state for reaction 4 is even more striking in its symmetry. The forming P–C bonds differ by only 0.014 Å while the other P–C bonds differ by the same amount. The bond orders for the P–C bond in each pair are also quite close. The bond path network shows a ring structure. Reaction 4 clearly goes through a synchronous transition state, in the sense that the two new bonds are formed to the same extent and the two P–C π-bonds are broken to the same extent. Both reactions 3 and 4 appear to follow the classic Woodward–Hoffmann allowed [$2\pi_s + 2\pi_a$] path. This is perhaps more evident in reaction 4, with its high symmetry, but the ring structure in **TS3** is compelling evidence for the [$2\pi_s + 2\pi_a$] path.

The difference in the reaction pathways between ketene and phosphaketene dimerization can be attributed to two major factors: ring strain and steric effects. The allowed [$2\pi_s + 2\pi_a$] path requires the two fragments to be oriented in perpendicular planes. We see this orientation in all four transition structures reported here, even in **TS1** and **TS2** which are not following the [$2\pi_s + 2\pi_a$] path. What forces the ketene dimerization to occur along an open geometry while phosphaketene follows a cyclic, synchronous path? A concerted [$2\pi_s + 2\pi_a$] reaction requires the formation of a ring structure in the transition state. For the ketene reaction, forming the ring structure adds sizable strain energy. This is avoided by first forming one C–C bond, followed by the second new bond and ring closure. This sequential reaction stage minimizes the activation energy. For phosphaketene, the added ring strain is much less than for the hydrocarbon analogue, due to the ability of phosphorus to accommodate small angles. A concerted reaction is thus not energetically disadvantaged. The concerted [$2\pi_s + 2\pi_a$] is unfavorable due to the steric interference in bringing the reaction systems together in the appropriate orientation. As seen in Scheme 3b, the substituents on the $2\pi_s$ fragment are directed toward the other fragment. With the short bond lengths involved in ketene dimerization, this steric interference cannot be overcome. The much longer C–P distances involved in phosphaketene dimerization, compared to the C–C distance in ketene dimerizations, reduce these steric interactions.

Conclusions

In agreement with previous experimental and theoretical studies, the dimerization of ketene appears to be kinetically controlled. Accurate evaluation of the energy difference between the two transition states leading to diketene and 1,3-cyclobutadione will require large basis sets and multireference CI calculations. Our best estimate (CCSD/D95*) is that **TS1** is 0.57 kcal mol^{-1} below **TS2**. The dimerization of ketene following either reaction 1 or 2 is asynchronous, with the near complete formation of a C–C bond before ring closure.

2,4-Diphospha-1,3-cyclobutanedione is the thermodynamic product (and may be the kinetic product) for the dimerization of phosphaketene. Surprisingly, this dimerization is only slightly exothermic. Both reactions 3 and 4 proceed by the classic [$2\pi_s + 2\pi_a$] pathway. Unlike the dimerization of ketene, a ring structure is present in the transition states **TS3** and **TS4**. Furthermore, reaction 4 is quite synchronous. The reduction in ring strain and steric interactions in the phosphaketene dimerization, relative to ketene dimerization, results in the Woodward–Hoffmann allowed [$2\pi_s + 2\pi_a$] dimerization of phosphaketene.

Acknowledgment is made to the donors of the Petroleum Research Fund, administered by the American Chemical Society, and the National Science Foundation for generous support of this research. Some of this work was supported by the National Center for Supercomputing Applications under Grant No. CHE940001N and utilized the Cray Y-MP at the National Center for Supercomputing Applications, University of Illinois at Urbana—Champaign.

(36) Nguyen, M. T.; Hegarty, A. F.; McGinn, M. A.; Ruelle, P. *J. Chem. Soc., Perkin Trans. 2* **1985**, 1991–1997.
(37) Manson, M.; Nakasi, Y.; Sunner, S. *Acta Chem. Scand.* **1968**, *22*, 171.